

Structural aspects of solid iodine associated with metallization and molecular dissociation under high pressure

K. Takemura* and S. Minomura

Institute for Solid State Physics, The University of Tokyo, Roppongi, Minoto-ku, Tokyo 106, Japan

O. Shimomura

National Institute for Researches in Inorganic Materials, Sakura-mura, Niihari-gun, Ibaraki 305, Japan

Y. Fujii and J. D. Axe

Brookhaven National Laboratory, Upton, New York 11973

(Received 8 February 1982)

The x-ray structure analysis of solid iodine has been made at room temperature and at various pressures up to 30 GPa, across the previously discovered phase-transition point $P_t=21$ GPa. In the low-pressure phase compression causes the nearest-neighbor intermolecular distance to approach the intramolecular one and the angle between the adjacent molecules to approach 90° . This structural change implies a significant increase of band overlapping which results in the metallization, well known in this system. The culmination of such structural trends in the low-pressure phase leads to a transition, at P_t , to a body-centered orthorhombic Bravais lattice formed upon dissociation into monatomic iodine. Atomic displacements in the low-pressure phase can be produced by dimerization, which is described by two displacement waves in the higher-symmetry high-pressure phase. A qualitative discussion on this transition has been made based on a Landau theory constructed by such a decomposition of displacements.

I. INTRODUCTION

Iodine is a typical elemental molecular crystal which undergoes an insulator-metal transition under pressure. The electrical resistance decreases gradually with pressure and reaches the metallic limiting value around 18 GPa.¹ The positive temperature coefficient of electrical resistance and the zero optical energy gap observed^{2,3} at 18 GPa reveal the metallic character of this material above this pressure. Lynch and Drickamer⁴ proposed two different models for its metallic conduction mechanism. One is the band overlap in molecular iodine, and the other is the unfilled conduction band resulting from a cubic Bravais lattice formed by monatomic iodine. In 1978 Shimomura *et al.*⁵ carried out high-pressure x-ray studies on iodine in its metallic state at 20.6 GPa by a sophisticated technique using a diamond-anvil cell and a position-sensitive detector. They found that the crystal structure at this pressure was the same as that at atmospheric pressure ($D_{2h}^{18}-Cmca$), and that iodine was still molecular. By using a similar technique, Takemura *et al.*⁶ discovered a new first-order phase transition at $P_t=21$ GPa and subse-

quently found the structure of the high-pressure (HP) phase above P_t to be a body-centered orthorhombic Bravais lattice ($D_{2h}^{25}-Immm$) formed by monatomic iodine.⁷ These results support the first model proposed by Lynch and Drickamer and confirm the molecular dissociation takes place after the metallization owing to band overlap is completed at about 18 GPa.

In the chemical bonding picture, such a metallization results from the increase of intermolecular charge transfer which is very sensitive to the intermolecular arrangement in a crystal. It is known from nuclear quadrupole resonance experiments⁸ that even at atmospheric pressure there is charge transfer, or a weak covalent bonding, between adjacent molecules in solid iodine. Furthermore, the following structural data at atmospheric pressure also suggest the presence of intermolecular covalent bonding: (1) The nearest-neighbor intermolecular distance (3.50 Å) is shorter than twice the van der Waals radius (4.30 Å), and (2) the bond length of an I_2 molecule in the crystalline state (2.70 Å) is longer than that in the gaseous state (2.67 Å). The latter fact shows that the intermolecular bond is formed at the expense of the in-

tramolecular bond. Thus the variation of intermolecular distances is expected to give important information on the charge transfer associated with the metallization process. However, the slight changes in atomic coordinates of iodine during metallization are very difficult to measure by conventional x-ray diffraction methods in the high-pressure region above 10 GPa. However, Shimomura *et al.*⁵ were able to detect the change in atomic coordinates of about 2% even at 20.6 GPa with a new high-pressure x-ray diffraction technique, which combines a diamond-anvil cell with a position-sensitive detector. A similar detector system further developed by Fujii *et al.*⁹ led the present authors to the discovery of a new phase transition at 21 GPa,⁷ and it has also enabled them to carry out the present detailed structural study on the metallization mechanism in this system.

II. EXPERIMENTAL DETAILS

The iodine sample, with purity of 99.8%, was obtained from Wako Pure Chemical Industries, Ltd. In order to make a fine powder, the sample was ground and mechanically crushed several times. The diamond-anvil cell used in the present experiments was the same as that in the previous experiments.^{6,7,10} The powdered sample was packed in a hole (0.30 mm in diameter, 0.15 mm deep) formed by a gasket made of Udimit 700. A small ruby chip for pressure measurement was glued onto the face of one of the anvils. No pressure transmitting fluid was used because iodine is soluble in alcohol mixtures. All handling of the sample was performed in an argon atmosphere to avoid chemical reaction. The pressure was determined by the wavelength shift of the ruby R_1 fluorescence line. The pressure distribution in the specimen was estimated to be ± 2 GPa at 30 GPa from the broadening of this line.

The x-ray diffraction experiments were carried out by a position-sensitive detector (PSD) developed for Mo $K\alpha$ radiation.⁹ The x rays emitted from a Mo target (Philips fine focus, 2 kW) were monochromatized with the (002) reflection of pyrolytic graphite. A specially-designed collimator system¹⁰ enabled the collimated x-ray beam (0.15 mm in diameter and 0.3° in angular divergence) to be centered with respect to the gasket hole so that no part of the gasket was hit by the beam. This is crucial to reduce the background and eliminate diffraction lines from the gasket. The uniform intensity of each diffracted ring was checked by taking

Debye-Scherrer photographs before measurement with the PSD to ensure the absence of any preferred orientation of the crystallites. The diffraction patterns were measured in the scattering angle range of $-40^\circ < 2\Theta < 40^\circ$, which was limited by an opening of a slot of the present diamond-anvil cell. The typical measuring time at one detector position covering about 20° was 12 h. Corrections for the natural background, inhomogeneous counting efficiency, and absorption were made when obtaining the integrated intensity of each diffraction peak.⁹ The angular resolution was 0.038° per channel in the present diffracton geometry.

III. EXPERIMENTAL RESULTS

A. Low-pressure phase (molecular phase)

Typical diffraction patterns of iodine in both insulator and metallic states in the low-pressure (LP) molecular phase below $P_t = 21$ GPa are shown in Figs. 1(a) and 1(b), respectively. The position and intensity of each diffracton peak were obtained by least-squares Gaussian fitting to its profile. Measurements were carried out at pressures of 3.3, 6.6, 10.2, 15.3, and 19.8 GPa. The parameters to be determined in the structure analysis based on the $8f$ sites in the space group $D_{2h}^{18}-Cmca$ were as follows: the atomic coordinates y and z [see Fig. 2(a)], an isotropic temperature factor B , and a scale

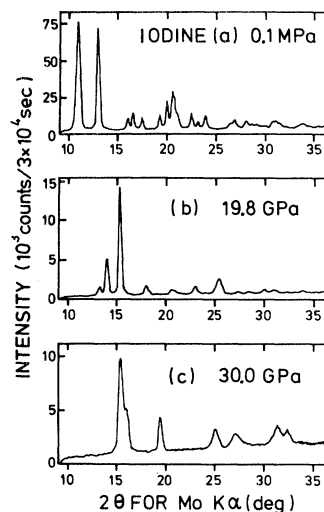


FIG. 1. X-ray diffraction patterns of iodine at (a) 0.1 MPa (LP, insulator state), (b) 19.8 GPa (LP, metallic state), and (c) 30.0 GPa (HP, monatomic phase). The pattern (a) was obtained from the sample before being enclosed in the diamond-anvil cell.

factor. They were obtained by least-squares fitting so as to minimize the χ^2 factor defined by

$$\chi^2 = \sum [(I_0^2 - I_c^2) / 2I_0\sigma_0]^2 / (N - P),$$

where I_0 and I_c are the observed and calculated intensities, σ_0 is the uncertainty of I_0 , and $N - P$ is the number of intensity data minus the number of parameters. The final values of the parameters and other related crystallographic data are listed in Table I. The reliability factor defined by

$$R = \sum |I_0 - I_c| / \sum I_0$$

was about 12% at each pressure.

As shown in the table, the atomic coordinate y increases with pressure, whereas z is nearly constant. In order to clearly see the molecular motion in the metallization process, we introduce the polar coordinates

$$r = [(by)^2 + (cz)^2]^{1/2}$$

and

$$\theta = \tan^{-1}(by/cz).$$

As shown in the same table, r is nearly constant but θ increases with pressure. The iodine molecule

rotates around the a_L axis with increasing pressure without appreciable change in the bond length. (Hereafter, subscripts L and H are used to represent the low- and high-pressure phases.) Such a movement can be seen in Figs. 2(a) and 2(b), which show the projection of atomic positions onto the a_L plane. The variation of the major interatomic distances with pressure is tabulated in Table I and also plotted in Fig. 3. The intermolecular distances r_{12} and r_{17} approach the intramolecular one r_{12} with increasing pressure. The volume compression calculated from the lattice constants is shown in Fig. 4. Previously, Bridgman reported an abrupt volume change of 2% at 1.3 GPa.¹² However, in the present x-ray experiment (with the 0.5% detectability for volume change), no discontinuous change was observed in that pressure range.

B. High-pressure phase (monatomic phase)

The present authors⁷ have already reported on the structure determination of the HP phase above P_t , based on the x-ray diffraction patterns taken at 30 GPa shown in Fig. 1(c). The crystal belongs to

TABLE I. Crystallographic data for the LP molecular phase of iodine at several pressures.

	0.1 MPa ^a	3.3	Pressure (GPa)			
			6.3	10.2	15.3	19.8
Lattice constants and volume						
a (Å)	7.136(10)	6.572(37)	6.337(26)	6.115(16)	5.938(10)	5.798(7)
b (Å)	4.686(7)	4.428(60)	4.292(43)	4.159(27)	4.043(18)	3.969(13)
c (Å)	9.784(15)	9.566(61)	9.423(46)	9.202(17)	9.152(14)	9.070(7)
V (Å ³)	327.2(15)	278.4(45)	256.3(30)	234.0(17)	219.7(11)	208.7(8)
Atomic coordinates						
y	0.1543(4)	0.172(4)	0.186(3)	0.198(7)	0.207(6)	0.214(6)
z	0.1174(1)	0.114(3)	0.116(3)	0.116(4)	0.115(3)	0.116(3)
r (Å)	2.715(6)	2.66(6)	2.71(5)	2.70(7)	2.70(5)	2.71(5)
θ (°)	32.2(1)	35.0(10)	36.2(9)	37.6(14)	38.4(11)	38.9(11)
Interatomic distances (Å)						
1-2	2.715(6)	2.66(6)	2.71(5)	2.70(7)	2.70(5)	2.71(5)
1-3	4.412(7)	4.19(4)	4.05(3)	3.93(5)	3.86(4)	3.78(4)
1-5	4.269(6)	3.96(2)	3.83(2)	3.70(1)	3.59(1)	3.51(1)
1-6	4.337(7)	4.00(4)	3.89(3)	3.75(5)	3.66(3)	3.59(3)
1-7	3.496(6)	3.42(5)	3.31(4)	3.22(6)	3.19(4)	3.14(4)
1-2'	3.972(6)	3.63(6)	3.47(4)	3.30(7)	3.17(5)	3.10(5)
Temperature factor						
B (Å ²)	anisotropic	4.1(6)	5.3(5)	6.3(14)	4.8(7)	4.6(6)

^aTaken from Ref. 11 ($T = 110$ K). Numbers in parentheses denote standard deviations.

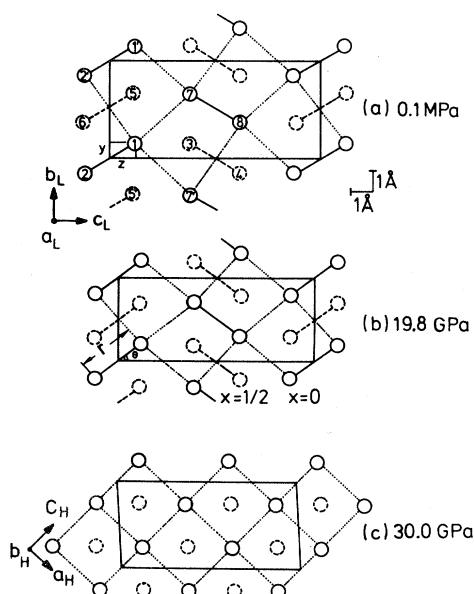


FIG. 2. Projection of the atomic positions of iodine at (a) 0.1 MPa, (b) 19.8 GPa, and (c) 30.0 GPa. The crystallographic unit cell of the LP phase is shown by the solid rectangle in (a) and (b) while that of the HP phase is shown by the dotted one in (c).

a body-centered orthorhombic (bct) lattice with the space group $D_{2h}^{25}-Immm$. The lattice constants at 30 GPa were determined as

$$a_H = 3.031 \pm 0.004,$$

$$b_H = 5.252 \pm 0.009,$$

and

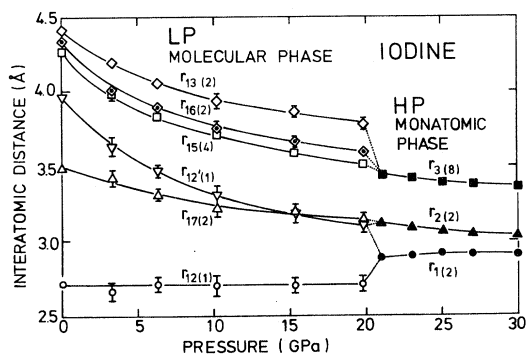


FIG. 3. Variation of interatomic distances with pressure for the LP molecular phase (open symbols) and for the HP monatomic phase (solid symbols). r_{ij} in the LP phase is the interatomic distance between atom i and j which are indicated in Fig. 2(a). The number in parentheses denotes the coordination number.

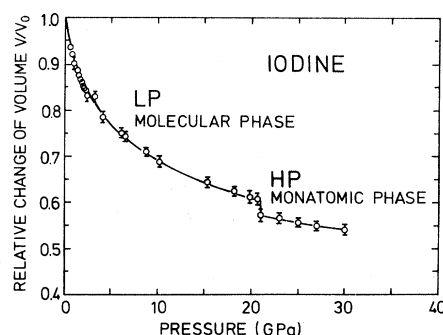


FIG. 4. Volume compression of iodine. The possible error in V/V_0 is shown by the vertical bar.

$$c_H = 2.904 \pm 0.009$$

as measured in Å. The following relationship holds between the crystal axes of the LP molecular phase and those of the HP monatomic phase;

$$\vec{a}_H = -\vec{b}_L/2 + \vec{c}_L/4,$$

$$\vec{b}_H = \vec{a}_L,$$

and

$$\vec{c}_H = \vec{b}_L/2 + \vec{c}_L/4.$$

The bct unit cell is drawn by the dotted lines in Fig. 2(c). Also shown in the same figure is the projection of the atomic positions onto the b_H plane at 30 GPa. Note that the crystal lattice is formed by monatomic iodines. This structure has the following features: An iodine atom in the b_H plane coordinates with 12 neighboring atoms, which are four atoms in the b_H plane (the first- and second-nearest neighbor) and eight atoms at the body-centered positions (the third-nearest neighbor). The second- and third-nearest-neighbor distances (r_2 and r_3) are longer than the first one (r_1) only by 4% and 16%, respectively. The variation of these near-neighbor distances with pressure is also shown in Fig. 3. The axial ratio a_H/c_H varies from 1.80 at 21 GPa to 1.04 at 30 GPa. The extrapolation of these data implies that the structure of the monatomic phase approaches a face-centered tetragonal lattice with $a_H/c_H = 1$ at higher pressure which is presumably accomplished at about 45 GPa. The volume compression of the HP phase was calculated from lattice constants and is shown in Fig. 4 together with that of the LP phase. The volume change at the structural phase transition at $P_t = 21$ GPa is 4%. The slopes of the compression curves in both phases are very similar near P_t .

IV. PHENOMENOLOGICAL THEORY OF DIMERIZATION

In the absence of a detailed microscopic understanding of this transition, some comments of a more phenomenological nature may be in order. This transition was found to be reversible⁶; therefore, the molecular dissociation taking place at P_t on compression can be regarded conversely as *dimerization* of iodine atoms of the HP phase with decreasing pressure. As shown in Fig. 5, the dimerization producing atomic displacements for the HP-to-LP transition decompose into two plane standing waves. The first (primary) wave is quasitransverse with wave vector $\vec{q}_1 = (\vec{a}_H^* + \vec{c}_H^*)/4$ with the displacements along \vec{b}_L . The secondary wave is quasilongitudinal (displacements along \vec{c}_L) with wave vector $\vec{q}_2 = 2\vec{q}_1$. The amplitudes of the two displacement waves η_1 and η_2 , defined by $\frac{1}{4} - y$ and $\frac{1}{8} - z$, respectively, are easily deduced from the positional parameters of the LP phase and are shown in Fig. 6 as a function of pressure.

This decomposition of the displacements can be used to construct a Landau theory of the phase transition. Defining the higher-symmetry HP phase to be the normal (i.e., untransformed) state, the change in the crystalline density function associated with the LP phase is described by three *order parameters*, Q_1 , Q_1^* , and Q_2 ($\eta_2 = |Q_2|$), as

$$\Delta\rho(\vec{r}) = Q_1 e^{i\vec{q}_1 \cdot \vec{r}} + Q_1^* e^{-i\vec{q}_1 \cdot \vec{r}} + Q_2 (e^{i\vec{q}_2 \cdot \vec{r}} + e^{-i\vec{q}_2 \cdot \vec{r}}).$$

Note that there are two independent primary wave vectors $\pm\vec{q}_1$, whereas $\vec{q}_2 = -\vec{q}_2$ (modulus a HP reciprocal-lattice vector) and is not independent, so that $Q_2^* = Q_2$. The first few terms of a Landau free-energy expansion are determined by translational invariance and are of the form:

$$F = \frac{1}{2}aQ_1Q_1^* + \frac{1}{2}bQ_2Q_2^* + \frac{1}{2}d(Q_1^2 + Q_1^{*2})Q_2 + \frac{1}{4}e(Q_1Q_1^*)^2 + \frac{1}{8}f(Q_1^4 + Q_1^{*4}) + \frac{1}{6}g(Q_1Q_1^*)^3 + \dots, \quad (1)$$

or on writing $Q_1 = \eta_1 e^{i\phi}$,

$$F = \frac{1}{2}a\eta_1^2 + \frac{1}{2}bQ_2^2 + d\eta_1^2 Q_2 \cos 2\phi + \frac{1}{4}(e + f \cos 4\phi)\eta_1^4 + \frac{1}{6}g\eta_1^6 + \dots. \quad (2)$$

Minimizing the free energy with respect to Q_2 , we find that

$$Q_2 = -(d/b)\cos^2\phi\eta_1^2. \quad (3)$$

Minimizing as well with respect to ϕ and replacing Q_2 and ϕ by their optimal values in Eq. (2), we arrive at a constrained free energy

$$\tilde{F}(\eta_1) = \frac{1}{2}a\eta_1^2 + \frac{1}{4}\tilde{e}\eta_1^4 + \frac{1}{6}g\eta_1^6 + \dots, \quad (4a)$$

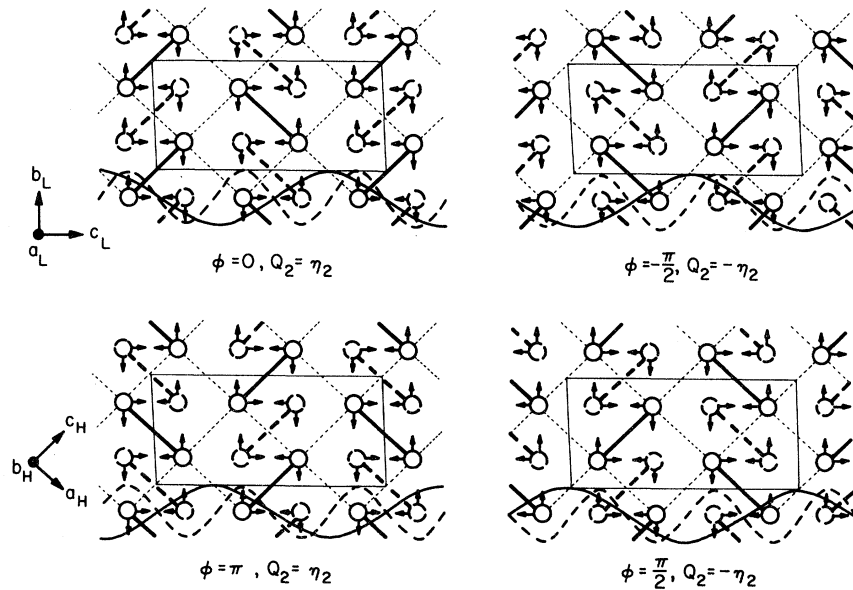


FIG. 5. Theoretically predicted four types of domains in the LP phase produced by dimerization for the HP-to-LP transition of iodine. Two displacement waves with wave vectors $\vec{q}_1 = (\vec{a}_H^* + \vec{c}_H^*)/4$ (transverse) and $\vec{q}_2 = 2\vec{q}_1$ (longitudinal) are drawn by solid and dashed curves, respectively.

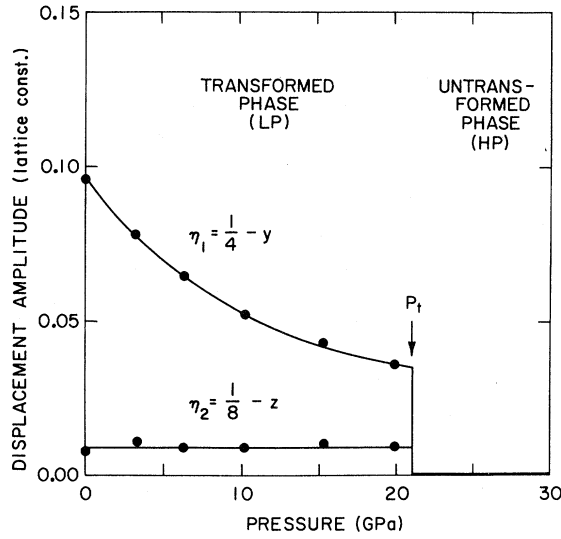


FIG. 6. Pressure dependence of displacement amplitudes of two-order parameter $\eta_1 = \frac{1}{4} - y$ and $\eta_2 = \frac{1}{8} - z$ experimentally obtained in the LP phase (circles). Solid lines are a guide for the eyes.

with

$$\tilde{e} = [e - |f| - 4(d^2/b)]. \quad (4b)$$

There are several qualitative features which can be deduced from the above development. The first observation is that Eq. (2) is invariant under the following replacements,

$$(\phi; Q_2) \rightarrow [\phi + n\pi/2; (-1)^n Q_2] \quad \text{for } n = 0, 1, 2, 3.$$

These solutions represent four distinct but identical degenerate LP configurations as shown in Fig. 5. We expect that all four types of domains coexist in the LP phase.

As is well known, Eq. (4a) describes either a continuous (second-order) transition if

$$a(P_t) = 0, \quad \tilde{e}(P_t) > 0, \quad g(P_t) > 0,$$

or a discontinuous (first-order) transition at

$$a(P_t) > 0 \quad \text{if} \quad \tilde{e}(P_t) < 0, \quad g(P_t) > 0.$$

Now consider primary wave vectors \vec{q} in the neighborhood of the commensurate value \vec{q}_1 . From Eq. (1), $f = 0$ unless $\vec{q} = \vec{q}_1$. Thus $\tilde{e}(\vec{q})$ is most negative (if it is negative at all near \vec{q}_1) for $\vec{q} = \vec{q}_1$. Thus commensurate, $\vec{q} = \vec{q}_1$, implies first-order and vice versa, because of the "lock-in" term $f(Q_1^4 + Q_1^{*4})$ in the free energy. More precisely, since $a(\vec{q})$ is not required by symmetry to be ex-

tremal for $\vec{q} = \vec{q}_1$ [in contrast to $b(\vec{q})$ around $\vec{q} = \vec{q}_2$, for example], we expect a continuous transition leads to an *incommensurate* LP phase, with \vec{q} having arbitrary direction (within the $\vec{a}_H - \vec{c}_H$ plane) and magnitude. Only for a first-order transition does the lock-in potential single out $\vec{q} = \vec{q}_1$.

It is certainly possible to make the above treatment quantitative by parametrizing the coefficients $a(P)$, $\tilde{e}(P)$, etc., to reproduce $\eta_1(P)$ and $\eta_2(P)$ from Fig. 6. However, such a parametrization suffers from lack of uniqueness, and we have thus far been unable to devise a compellingly simple scheme which recommends itself among the possibilities. An alternative and entirely different approach to the statistical-mechanical aspects of the transition which may merit further study, is the possibility of a mapping onto an n -vertex model,¹³ one variant of which is the so-called "dimer model" and for which numerous exact results exist in two dimensions.

V. DISCUSSION

Based on the present structure analysis of the LP phase of iodine, the metallization process can be explained as follows: A covalent bond is formed by the charge transfer of lone-pair $5p$ electrons, for example, between the $5p_x$ orbital of atom 7 and vacant $5p_z$ orbital of atom 1 [Fig. 2(a)]. Similar charge transfer exists between atoms 1 and 7', which results in a network of charge transfer formed in the a_L plane. This network gives rise to the observed isotropic electrical conductivity in this plane. As pressure is applied, the intermolecular distances decrease as observed in the present study; therefore, the charge transfer increases continuously resulting in the gradual decrease in electrical resistivity. Since such an intermolecular charge transfer is formed at the expense of the intramolecular I_2 bond, the increase in the charge transfer is expected to decrease the strength of the intramolecular bonding. However, neither the present experiment nor the recent Raman scattering experiment¹⁴ showed appreciable change in the intramolecular distance or the frequency of the bond stretching mode. The iodine molecule behaves like a rigid molecule only rotatable around the a_L axis. The energies of solid iodine in various molecular configurations are now calculated by Kiichi¹⁵ by the use of a self-consistent-field tight-binding approximation.

The band calculations of iodine at both atmospheric pressure and 19.8 GPa were recently carried

out by Natsume¹⁶ based on the pseudopotential method with a plane-wave approximation. According to his results, the band structure is almost symmetric about the k_x axis, perpendicular to the a_L plane. The energy gap of 1.3 eV calculated at atmospheric pressure agrees well with the observed value from optical absorption.³ At 19.8 GPa the valence and the conduction bands overlap at different points in \vec{k} space, which suggest a semimetallic character. The Fermi surface is supposed to consist of an ellipsoid of holes at the Γ point and two separated shells of electrons around the ellipsoid. The ellipsoid and two shells are elongated in the direction of the k_x axis. This Fermi surface implies that the mobility of holes and electrons is very low in the direction of k_x while it is high in the k_x plane (molecular plane). Namely, iodine at 19.8 GPa is characterized as a pseudo-two-dimensional semimetal which has higher conductivity in the molecular plane.

As pressure is increased in the LP phase, the intermolecular distances become close to the intramolecular one, and the angle between two adjacent molecules approaches 90° [Fig. 2(b)]. The culmination of these trends results in the HP structure formed by monatomic iodines. From a structural point of view, the HP phase is nearly isotropic in the b_H plane but it is anisotropic in the direction perpendicular to the b_H plane. The electrical conduction is also anisotropic. A preliminary band calculation at 30 GPa also by Natsume¹⁶

has suggested an important role by hole conduction in this phase.

The molecular dissociation and the large volume reduction observed at P_t might result in a dramatic anomaly in some other physical quantities. In all of the previous works on iodine, however, no such anomaly has been reported. Recently, Sakai *et al.*¹⁷ carried out precise measurements of electrical resistance at room temperature by using a specially designed diamond-anvil cell, and found only a small increase at about 21 GPa.

Based on the present structural data in both LP and HP phases of solid iodine, further theoretical study of its electronic structure and phase transition is desired in order to clarify the mechanism of the metallization and molecular dissociation, or dimerization, from a microscopic point of view.

ACKNOWLEDGMENTS

The authors greatly appreciate Y. Natsume of Chiba University for his kind communications to us of his band calculations prior to publication. They are also grateful to T. Kiichi of Osaka University for his valuable discussion. The present work was supported by the Grant-in-Aid for Scientific Research from the Ministry of Education in Japan. Work at Brookhaven was supported in part by the U. S. Department of Energy under Contract No. DE-AC02-76CH00016.

*Present address: Physikalisches Institut, Lehrstuhl III, der Universität Düsseldorf, 4000 Düsseldorf, West Germany.

¹A. S. Balchan and H. G. Drickamer, *J. Chem. Phys.* **34**, 1948 (1961).

²B. M. Riggelman and H. G. Drickamer, *J. Chem. Phys.* **37**, 446 (1962).

³B. M. Riggelman and H. G. Drickamer, *J. Chem. Phys.* **38**, 2721 (1963).

⁴R. W. Lynch and H. G. Drickamer, *J. Chem. Phys.* **45**, 1020 (1966).

⁵O. Shimomura, K. Takemura, Y. Fujii, S. Minomura, M. Mori, Y. Noda, and Y. Yamada, *Phys. Rev. B* **18**, 715 (1978).

⁶K. Takemura, Y. Fujii, S. Minomura, and O. Shimomura, *Solid State Commun.* **30**, 137 (1979).

⁷K. Takemura, S. Minomura, O. Shimomura, and Y. Fujii, *Phys. Rev. Lett.* **45**, 1881 (1980).

⁸C. H. Townes and B. P. Dailey, *J. Chem. Phys.* **20**, 35

(1952).

⁹Y. Fujii, O. Shimomura, K. Takemura, S. Hoshino, and S. Minomura, *J. Appl. Crystallogr.* **13**, 416 (1980).

¹⁰K. Takemura, O. Shimomura, K. Tsuji, and S. Minomura, *High Temp. High Pressures* **11**, 311 (1979).

¹¹F. van Bolhuis, P. B. Koster, and T. Michelsen, *Acta Crystallogr.* **23**, 90 (1967).

¹²P. W. Bridgman, *Phys. Rev.* **48**, 893 (1935).

¹³See, for example, E. H. Lieb and F. Y. Wu, in *Phase Transitions and Critical Phenomena*, edited by C. Domb and M. S. Green (Academic, New York, 1972), Vol. I.

¹⁴O. Shimomura (private communication).

¹⁵T. Kiichi (private communication).

¹⁶Y. Natsume (private communication).

¹⁷N. Sakai, K. Tsuji, K. Takemura, T. Kajiwara, and S. Minomura (private communication).